Available online at www.sciencedirect.com

SciVerse ScienceDirect

www.elsevier.com/locate/matchar

Increasing Ti–6Al–4V brazed joint strength equal to the base metal by Ti and Zr amorphous filler alloys

E. Ganjeh[a,*], H. Sarkhosh[b], M.E. Bajgholi[c], H. Khorsand[a], M.H. Ghaffari[d]

[a]Materials Division, Faculty of Mechanical Engineering, K.N. Toosi University of Technology, Tehran, Iran
[b]Faculty of Biomedical Engineering, Amirkabir University of Technology, Tehran, Iran
[c]Department of Material Engineering, Science and Research Branch, Islamic Azad University, Tehran, Iran
[d]Department of Electrical and Electronics Engineering, UNAM – National Institute of Materials Science and Nanotechnology, Bilkent University, Ankara 06800, Turkey

ARTICLE DATA

Article history:
Received 1 April 2012
Received in revised form 29 April 2012
Accepted 30 May 2012

Keywords:
Furnace brazing
Ti–6Al–4V alloy
Microstructure
Mechanical properties
XRD analysis

ABSTRACT

Microstructural features developed along with mechanical properties in furnace brazing of Ti–6Al–4V alloy using STEMET 1228 (Ti–26.8Zr–13Ni–13.9Cu, wt.%) and STEMET 1406 (Zr–9.7Ti–12.4Ni–11.2Cu, wt.%) amorphous filler alloys. Brazing temperatures employed were 900–950 °C for the titanium-based filler and 900–990 °C for the zirconium-based filler alloys, respectively. The brazing time durations were 600, 1200 and 1800 s. The brazed joints were evaluated by ultrasonic test, and their microstructures and phase constitutions analyzed by metallography, scanning electron microscopy and X-ray diffraction analysis. Since microstructural evolution across the furnace brazed joints primarily depends on their alloying elements such as Cu, Ni and Zr along the joint. Accordingly, existence of Zr_2Cu, Ti_2Cu and $(Ti, Zr)_2Ni$ intermetallic compounds was identified in the brazed joints. The chemical composition of segregation region in the center of brazed joints was identical to virgin filler alloy content which greatly deteriorated the shear strength of the joints. Adequate brazing time (1800 s) and/or temperature (950 °C for Ti-based and 990 °C for Zr-based) resulted in an acicular Widmanstätten microstructure throughout the entire joint section due to eutectoid reaction. This microstructure increased the shear strength of the brazed joints up to the Ti–6Al–4V tensile strength level. Consequently, Ti–6Al–4V can be furnace brazed by Ti and Zr base foils produced excellent joint strengths.

1. Introduction

The importance of titanium alloys has been increasing due to structural demands for aerospace and medical applications [1]. Titanium and its alloys have two allotropic phases, low temperature hexagonal α phase and high temperature body-centered cubic β phase. This transformation from α to β is known as the β-transus temperature. The alloying elements of titanium, depending on their influence on the β-transus temperature, are classified as neutral, α-stabilizers and β-stabilizers. Among the α-stabilizers, aluminum is the most important alloying element. The α-stabilizing elements are subdivided into β-isomorphous and β-eutectic elements. The most important β-isomorphous elements are Mo and V, due to their much higher solubility in titanium. On the other hand, even very low volume fractions of β-eutectic elements, such as Ni, Cu, Fe, Mn and Cr, can lead to the formation of intermetallic compounds. Sn and Zr are considered as neutral elements since they have (nearly) no influence on the titanium microstructure. However, as far as strength is concerned, they are not neutral since they primarily strengthen

* *Corresponding author at:* No. 15-19, Pardis Street, Mollasadra Avenue, Vanak Square, Tehran, P.O. Box 19395-1999, Iran. Tel.: +98 2188674741.
E-mail address: navidganjehie@sina.kntu.ac.ir (E. Ganjeh).

1044-5803/$ – see front matter © 2012 Elsevier Inc. All rights reserved.
doi:10.1016/j.matchar.2012.05.016

the α-phase. Usually titanium alloys are classified as α, α+β, and β alloys, with further subdivision into near α and metastable β alloys [2–4].

For the last half of the twentieth century, Ti–6Al–4V has accounted for about 45% of the total weight of all titanium alloys shipped. During the approximately 60 years that titanium has been commercially available, the Ti–6Al–4V alloy has captured almost 50–60% of the market share [2,5]. Ti–6Al–4V belongs to a type of α–β duplex titanium alloys, since their microstructure can be tailored to provide either high toughness at ambient temperature or high creep resistance at elevated temperatures. It is one of the most important titanium alloys for aerospace, turbine engines and biomedical applications owing to their highly desirable performance characteristics, such as high strength-to-weight ratio, low density, and corrosion resistance [6]. When compared with stainless steel, nickel and aluminum alloys operating within the same temperature range, its specific strength ratio is significantly higher [2,7–9].

One of the main processing stages in any industry is the method of joining. Welding and brazing are used routinely and successfully in joining titanium and its alloys. Welding usually impacts the materials properties at the so-called heat affected zone (HAZ). In contrast, brazing has less impact on the mechanical properties of the base material. Brazing is one of the most useful techniques employed for joining ceramics to metals [10]. Brazing has been extensively applied for joining titanium and titanium alloys [1,11–14]. Joining of titanium alloys has to be performed in an inert gas or high-vacuum atmosphere with stringent process controls to avoid reaction of titanium with other elements. Filler alloys with brazing temperatures below the β-transus are preferable because they preserve and provide high mechanical properties of titanium brazed assemblies. It is preferred that the brazing temperature of α–β titanium alloys not to exceed the β-transus temperature [6]. This varies from 980 to 1040 °C for Ti–6Al–4V to obtain the fine equiaxial duplex microstructure for optimal mechanical properties. Ti or Zr base brazing fillers provide high joint strength and good corrosion resistance when compared to the other types of brazing fillers such as Ag or Al base fillers [12,14,15].

Ti–15Cu–15Ni (wt.%) and Ti–15Cu–25Ni (wt.%) are two commercially available Ti-based braze alloys. However, brazing temperatures of Ti–Cu–Ni fillers can be lowered with the addition of Zr. Generally, the melting points of the Ti–Cu–Ni–Zr amorphous fillers are approximately 100 °C lower than those of the conventional titanium-based fillers. Therefore, using these fillers makes it possible to braze the Ti–6Al–4V alloy at a temperature below its β-transus temperature [16].

Chang et al. [15] investigated the effects of brazing parameters on the strength of brazed joints between Ti–6Al–4V and Ti–15V–3Al–3Cr–3Sn (β- phase alloy) by both infrared and furnace brazing using Ti–15Cu–15Ni and Ti–15Cu–25Ni filler foils. They concluded that brazing at 970 °C and soak time of 180 s resulted in Ti-rich and Cu–Ni-rich phases in the center of the brazed zone, which caused lower shear strength at the joints. Higher brazing temperatures and/or longer soak durations resulted in the diminishing of the Cu–Ni-rich phase, leaving behind the ductile Ti matrix. Using Ti–15Cu–15Ni filler foil and optimal parameters (970 °C–1200 s), they reported average shear strength of around 528 MPa and occurrence of fracturing at the base material.

In this study, furnace brazing in an argon atmosphere (inert gas) was applied to join Ti–6Al–4V alloy using brazing filler alloys STEMET 1228 (Ti–26.8Zr–13Ni–13.9Cu, wt.%) and STEMET 1406 (Zr–9.7Ti–12.4Ni–11.2Cu, wt.%). Using argon atmosphere instead of high-vacuum condition should make the process more economic and gives this possibility to be applicable in industrial applications. The correlation of temperature and time on the microstructural development and performance of Ti–6Al–4V brazed joints has been studied.

2. Experimental Procedures

Plates of Ti–6Al–4V alloy (ASTM Grade 5) of 3 mm thickness with 1015 °C, α→β transformation (β-transus) were used as the base material. Chemical composition of the base material is given in Table 1. The ultimate tensile strength and elongation of our Ti–6Al–4V base material were 1010 MPa and 14%, respectively. Single lap shear specimens with 10 mm width in the reduced cross-section were prepared by means of a wire-cutting machine and then brazed with overlapping 9 mm (3 T) according to the JIS (Japanese Industrial Standard) Z 3192 [17] standard. It is recommended to use a lap width of not more than thrice the thickness of the base metals to achieve high strength for the joint [18]. Additionally, some plates measuring 15×10×3 mm^3 were brazed for the purpose of joint microstructure observation. For both STEMET 1228 ($T_{L/S}$=664/825 °C) and STEMET 1406 ($T_{L/S}$= 725/900 °C), 50 μm thick foils were used for brazing. All joining surfaces were polished by SiC papers up to grit 600, and ultrasonically cleaned by acetone for 1200 s at 50 °C prior to brazing. The brazing foils were cleaned in acetone before brazing and then sandwiched between the overlapping areas of the base material. The furnace used in this study was an atmosphere controlled furnace. Furnace brazing (Iranian patent number: 72122) was conducted in an argon atmosphere control. At first, the chamber was evacuated for about 600 s and then purged with high purity argon gas at a static flow which was controlled by a volume manometer. Thermocouple (Chromel–Alumel) was connected to the samples proximity to the lap joint area (hot zone). The heating and cooling rates during the brazing cycles were adjusted at~1 °C/s. The setting up and procedures of the brazing process have been described in our previous publication [19].

All brazing temperatures employed in this experiment were lower than the β-transus, as illustrated in Fig. 1. The joints were fixed with a steel clamp and then carefully placed inside the furnace. The process variables used in this study are listed in Table 2.

Table 1 – Chemical composition (wt.%) of the Ti–6Al–4V used in this experiment.

Alloy	Al	V	Cr	Cu	Fe	Mn	Mo	Nb	Sn	Zr	Si	Ti
Ti — ASTM B265 (Grade 5)	6.25	3.70	<0.01	<0.02	0.01	0.01	<0.3	0.02	<0.05	<0.01	0.02	Bal.

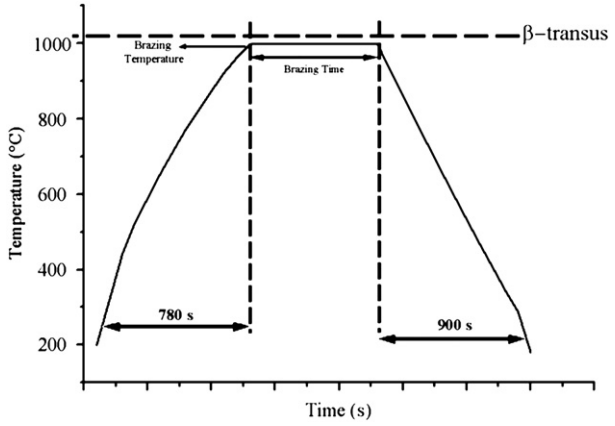

Fig. 1 – The furnace heating/brazing/cooling cycle used in this study.

After brazing the shear specimens, ultrasonic test was carried out using a probe generating a longitudinal wave of 22 MHz. Thickness measurement "Krautkramer Branson" was performed according to the AWS (American Welding Society) C3.8 [20]. To minimize the impact of contact pressure on the PAW amplitude, a thin layer of high-viscosity couplant was used. Sample preparation by standard grinding and polishing procedure was applied, and Kroll's reagent (3 ml HF, 6 ml HNO_3 and 100 ml H_2O) [21] was used for microstructure characterization. Cross sectional area examinations were performed using a light optical microscope (IMI-420) and a scanning electron microscope (VEGA/TESCAN). Compositions of the joining zone and the base materials near the joining zone were determined with an energy dispersive spectroscope (Rontec). The operational voltage was kept at 20 kV and its minimum spot size was approximately 1 μm.

The joined single overlap samples were shear tested in order to obtain the room temperature shear strengths of the resulting joints. The test was carried out by a Zwick/Reoll Hct 400/25 dynamic testing machine with a constant crosshead speed of $8.3\times10^{-4}\ s^{-1}$ [12,15]. After the shear test, load–displacement diagrams were obtained. Therefore by converting the load to stress and displacement to strain, stress–strain curves were gained. Two shear test specimens were performed for each brazing condition. So, the ± symbol points out to the standard deviation (SD) for shear strength and elongation. The applied stress during the shear test is focused entirely on the brazed joint, but this stress is focused on the base metal during the tensile test. Therefore, the shear test is a more applicable test to evaluate the mechanical properties of the brazed joints, in comparison with the tensile test [22].

Microhardness in the scale of HV0.1, performed for selective samples. Microhardness measuring was started from the base material and continuing each ~20 μm for 7 points up to the next BM. The microhardness testing technique followed the ASTM (American Society for Testing and Materials) E 384 [23] standard test method utilizing a Vickers diamond indenter (Wolpert/Instron) with a dwell time of 35 s. The microhardness values were carried out for three times in each point. Therefore, the mean value was taken for the present investigations in order to assure the repeatability and validity of the results. X-ray diffraction analysis (Philips PW 1800 diffractometer) was carried on fractured surface of samples to identify different phases. The scan range of 2θ was from 20 to 110° and the step size was 0.02°/s.

Table 2 – Summary of furnace brazing variables used in this research.

Filler braze alloys	STEMET 1228	STEMET 1406
Solidus/liquidus temperature (°C)	664/825	680/895
Furnace brazing temperature (°C)–time (s)	900–600	900–600
	900–1800	900–1800
	950–600	950–600
	950–1200	950–1800
	950–1800	990–600
		990–1200
		990–1800

3. Results and Discussion

3.1. Ultrasonic Test

Brazing was performed for all the planned combinations of temperatures and time durations. Sound joints seem to be without any defects like voids or cracks according to the ultrasonic test, for samples brazed with STEMET 1228 only at temperature of 950 °C and 990 °C for samples brazed with STEMET 1406, as demonstrated in Table 3. Therefore, the rest of this study was focused only on these two temperatures.

3.2. Microstructure Evolution

Optical micrographs of brazed joints at 950 °C with STEMET 1228, and at 990 °C with STEMET 1406, but for three different time durations of 600, 1200 and 1800 s are shown in Fig. 2. This photograph reveals the microstructural transition from the base material through the brazed joint. In the 600 s samples, the cross-sectional microstructures consist of three layers. With increase in brazing time, however, the microstructures clearly indicate progressive change, especially in the brazing time of 1800 s. In addition, there are some reaction layers between the brazing fillers and the Ti–6Al–4V base material, whose thicknesses have grown with the brazing time. The growth of the interfacial layers is a result of interdiffusion of the alloying

Table 3 – Results of ultrasonic tests for brazed joints.

Braze alloy	Temp. (°C)	Time (s)	Layer thickness (mm)	Joint thickness (mm)	Results
STEMET 1228	900	600	2.9	2.8	☐Acc. ☑Rej.
	900	1800	3.0	2.9	☐Acc. ☑Rej.
	950	600	3.0	5.7	☑Acc. ☐Rej.
	950	1200	2.9	5.9	☑Acc. ☐Rej.
	950	1800	3.1	6.0	☑Acc. ☐Rej.
STEMET 1406	900	600	3.0	3.0	☐Acc. ☑Rej.
	900	1800	2.9	2.8	☐Acc. ☑Rej.
	950	600	2.9	2.8	☐Acc. ☑Rej.
	950	1800	2.9	2.9	☐Acc. ☑Rej.
	990	600	3.1	5.8	☑Acc. ☐Rej.
	990	1200	2.8	6	☑Acc. ☐Rej.
	990	1800	3.0	5.9	☑Acc. ☐Rej.

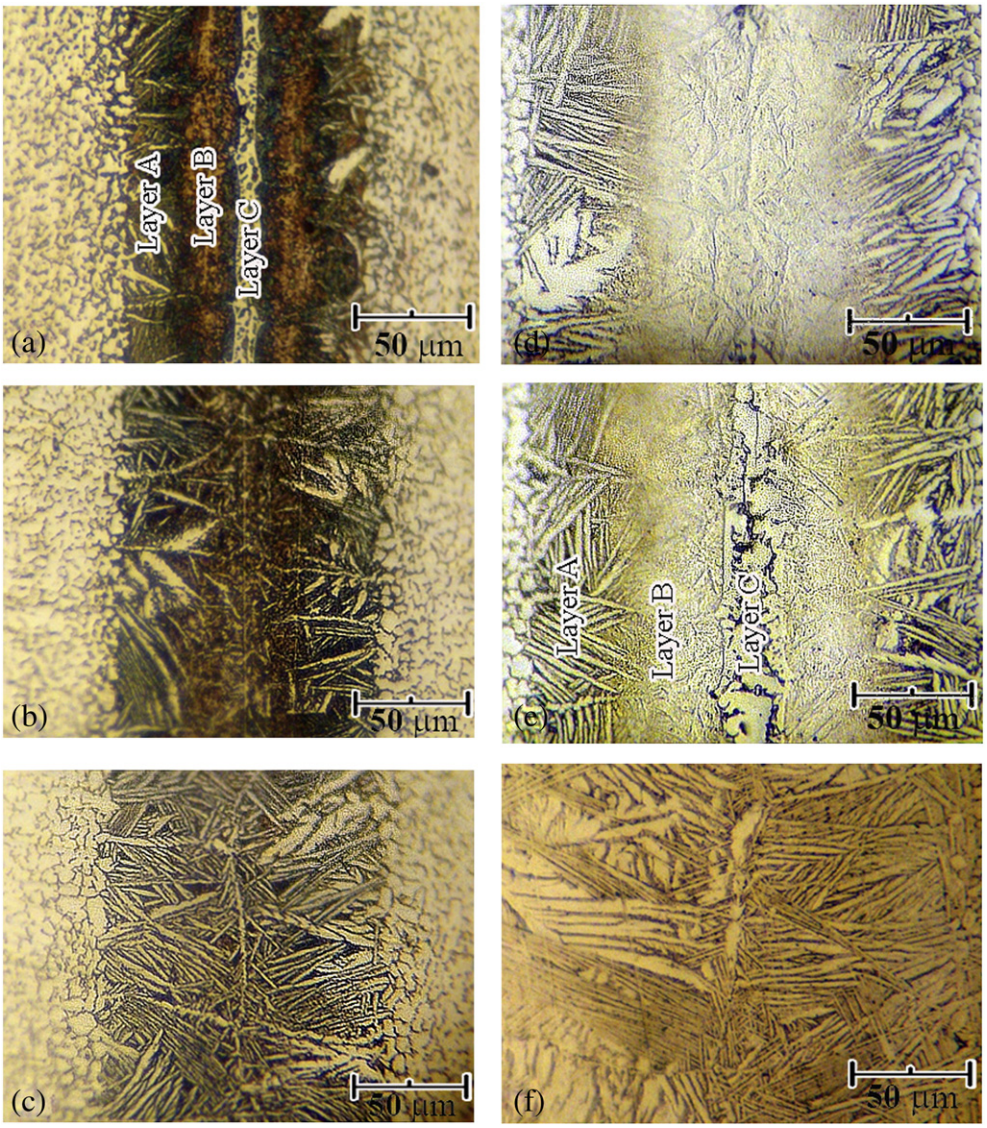

Fig. 2 – Microstructure of the brazed joints with STEMET 1228 at 950 °C for (a) 600, (b) 1200, and (c) 1800 s and STEMET 1406 at 990 °C for (d) 600 (e) 1200, and (f) 1800 s.

elements of the brazing fillers and the base material as discussed below.

During cooling from brazing temperature, plate-like α phase (light) nucleates and grows, out of the β phase (dark) at the base material. The structure of Ti–6Al–4V base material in the vicinity of layer A, consisting of equiaxed α (light) and intergranular β (dark) phases, coarsens slightly during the brazing treatment. Layer B is the inter-diffusion zone; during brazing, diffusion of Zr, Cu and Ni atoms from the molten filler into the base material transforms its structure into β phase. Layer C is where the original filler featureless structure has relatively remained intact as manifested in the optical microscopic level of Fig. 2. Finally, as the brazing soak time increases, the remaining filler material diffuses completely into the joint and disappears, leaving behind/producing the final lamellar α+β Widmanstätten structure [24].

For accurate recognition and characterization of the reaction layers at brazed joints, scanning electron microscope (SEM) backscattered electron imaging (BEI) of the transition regions of the joints was performed at various brazing conditions as shown in Figs. 3 and 4 for STEMET 1228 and STEMET 1406, respectively. Moreover, energy dispersive spectroscope (EDS) chemical analysis results of the different regions are provided in Tables 4 and 5, respectively. At the brazing duration of 600 s, several separate phases were generated. Based on the microstructural features and the chemical composition analysis from different phases, the brazed joints consisted of three regions as mentioned earlier. The formation of these regions indicated that a strong reaction between the molten filler and the Ti–6Al–4V base material must have occurred during brazing cycle. Different intermetallic compounds and transient secondary phases such as $(Ti,Zr)_2Ni$ or $(Ti,Zr)_2Cu$ took shape in the brazed joints with microstructural variants of the original α and β phases [25]. The decomposition of β phase in titanium alloys can take place by eutectoid transformations, and this frequently happens in the α–β alloys. The thickness of the eutectoid

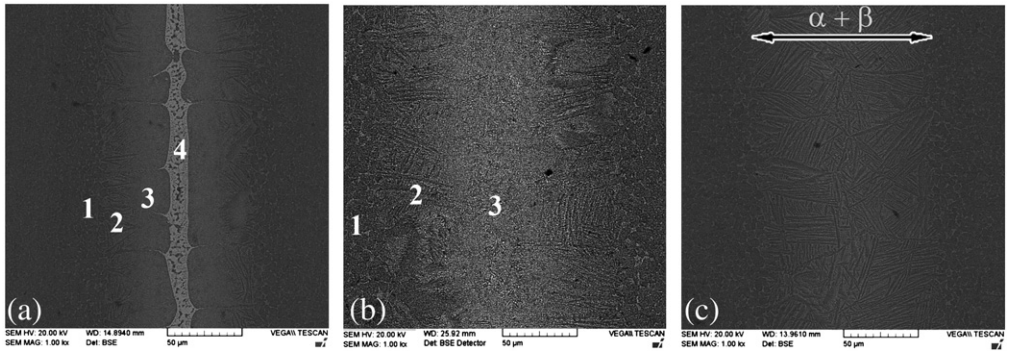

Fig. 3 – SEM BEIs of furnace brazed Ti–6Al–4V/STEMET 1228 specimens with various brazing conditions: (a) 950 °C–600 s, (b) 950 °C–1200 s and (c) 950 °C–1800 s.

regions increases with the increasing brazing time. It is suggested [12,16] that these phases should be the results of the reaction of dissolving elements of base material with Cu, Ni and Zr elements of the liquid filler alloy. The β to α transition is responsible for an acicular (plate-like) structure in titanium alloys [2]. During cooling, the size of α colonies as well as the thickness of the individual α plates become larger. The α colonies grow toward the braze joint but cannot fill the whole joint. Similarly, colonies grow on the interface of other colonies. To minimize the overall elastic strains, the new α plates growing by point contact on the broad faces of the existing α plates and tend to grow nearly perpendicular to those plates. This selective nucleation and growth mechanism in combination with a few number of α plates within the colonies lead to a typical microstructure called "basket weave", Widmanstätten or acicular structure [4]. The needle like (plate like) feature is the effect of rapid cooling (1 °C/s) from brazing temperature to room temperature. The formation of the acicular structure in both joints can be explained by the isothermal solidification that occurred during brazing. At the early stage of brazing, the Ti–6Al–4V base material dissolved/diffused considerably into the molten Ti or Zr base fillers. As a result, the molten filler in the vicinity of the Ti–6Al–4V base material became richer in Ti. The primary phase, which solidified isothermally, was the α-Ti rather than the β-Ti, when the brazing temperature was sufficiently lower than the β transus. During brazing, diffusion of the filler elements (Zr, Cu and Ni) into the base material was driven by the concentration gradients of these elements. However, the diffusion rates of Zr, Cu and Ni in α-Ti may be slow given that α-Ti has a close-packed crystal structure [2]. According to Ti–Cu and Ti–Ni binary alloy [26] phase diagrams (Fig. 5), maximum solubilities of Cu and Ni in β-Ti (13.5 and 10 at.%, respectively) are much more than those in α-Ti. So, these elements act as β-Ti stabilizers. Therefore, the α-Ti phase nucleated and grew into the joints, while the excessive Cu and Ni atoms were expelled from the growing α-Ti phase and segregated at the intercellular regions. Moreover, the disappearance of the segregated center regions was due to the interdiffusion of these filler elements within the joints and into the base material, i.e., this region completely diminished at the higher brazing duration of 1800 s due to the enhanced diffusion of Zr, Cu and Ni.

The most important general result obtained after brazing under different conditions is the absence of any changes in the base material microstructure. In particular, the absence of grain growth indicates that no overheating occurred in the base material. Therefore, the brazing temperature and time employed in this study were quite appropriate.

The model for describing diffusion in the brazing process is illustrated schematically in Fig. 6 [27]. When two base material pieces are joined together using one of the two brazing fillers, as shown in Fig. 6a, during the brazing process the filler melts but the base material pieces remain solid. After the filler melts, there is some dissolution of the base material into the liquid pool, and so the liquid initially becomes wider (Fig. 6b). Simultaneously, some atoms of Zr, Cu and Ni diffuse into the

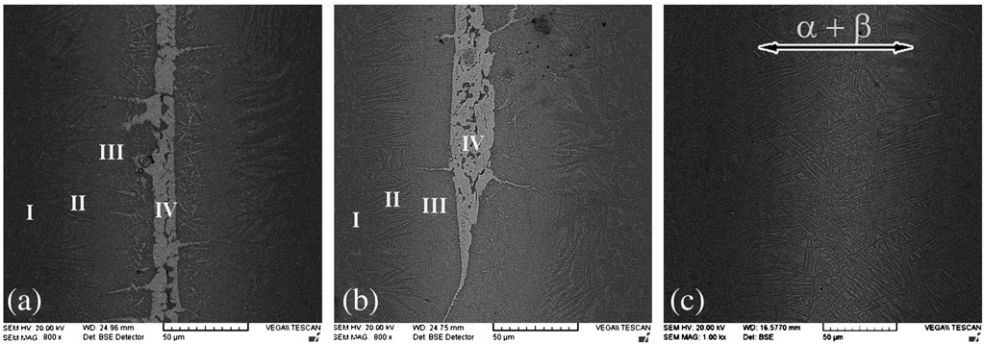

Fig. 4 – SEM BEIs of furnace brazed Ti–6Al–4V/STEMET 1406 specimens with various brazing conditions: (a) 990 °C–600 s, (b) 990 °C–1200 s and (c) 990 °C–1800 s.

Table 4 – Chemical analysis at regions shown in Fig. 3.

Symbol	Chemical analysis, at.%						Probable Phase
	Ti	Al	V	Zr	Ni	Cu	
1	85	6.2	3.7	1	2	2.1	Equiaxed α+β phase (Ti–6Al–4V)
2	78.6	9.7	2.3	2.1	4.9	2.4	Acicular α+β Ti
3	76.8	6.2	0.3	3.7	6	7	(α-Ti)+Cu–Ni in Ti-rich
4	54.5	2.9	1	12.4	14	15.2	$(Ti,Zr)Cu_2$, $(Ti,Zr)_2Ni$, $(Ti,Zr)_2Cu$

Table 5 – Chemical analysis at regions shown in Fig. 4.

Symbol	Chemical analysis, at.%						Probable Phase
	Ti	Al	V	Zr	Ni	Cu	
I	84.7	7.4	1.4	0.3	0.6	5.6	Equiaxed α+β phase (Ti-6Al-4V)
II	76.4	4.8	4.5	3.6	3.5	7.2	Acicular α+β rich Ti
III	81.4	4.5	1	1.1	1.8	10.2	(α-Ti)+Cu in Ti-rich
IV	39.7	6.6	0.9	13.6	11.2	28	$(Ti,Zr)Cu_2$, $(Ti,Zr)_2Ni$, $(Ti,Zr)_2Cu$

base material (Fig. 6c). Normally, liquids re-solidify only when cooled, but here the compositional changes occurring during diffusion bonding allow re-solidification of the joint while being held at a constant temperature. After the isothermal solidification is complete, atoms of alloying elements in filler alloy continue to diffuse (Fig. 6d), and the result will be a homogenized joint (Fig. 6e), possessing very similar mechanical properties to the base material.

3.3. *Mechanical Properties*

Fig. 7(a) shows the stress–strain curves for the room temperature shear tests of the brazed samples with STEMET 1228 at 950 °C for 600, 1200 and 1800 s. The yield and shear strengths along with elongation measures are presented in Fig. 7(b). The results revealed that the shear strength increased with increasing brazing time, and the joints fractured in the base material only for the brazing time of 1800 s. Different microstructural feature are responsible for different joint strengths and these are dependent extremely on brazing parameters (e.g. time, temperature and composition of filler alloy). The thickness and type of the reaction layers among the base material and brazed alloy are critical factors in determining the strength of the joints. It is well known that high-temperature brazing of Ti causes the formation of the high strength Widmanstätten joint structure in due time. However, at the shorter brazing times, the failure occurred within the central brazed (segregated) layer with lower strength (403 MPa) but higher elongation. It shows the maximum elongation generated at this condition. It was found from these results that the central brazed layer consists of brittle intermetallic compounds such as $(Ti,Zr)_2Ni$ and $(Ti,Zr)_2Cu$, causing lower shear strengths at the joints. Therefore, in order to obtain shear strength at the brazed joints comparable to the base material, disappearance of the central brazed layer consisting of brittle intermetallic compounds and the formation of Widmanstätten structure is necessary [12,16]. Results for the samples with STEMET 1406 at 990 °C for 600, 1200 and 1800 s are presented in Fig. 8. Similar to the previous case (STEMET 1228); increasing the brazing time was the main factor for the elevated joint strength, causing fracture propagation in the base material instead of the brazed joint. Segregation of the alloying elements (Zr–Cu–Ni) in the braze center region deteriorates the mechanical bonding strength of the brazed joints [15,16,28]. It is well known that the shear strength is 0.577 [29] of maximum tensile strength. Consequently, the perfect brazing temperature was determined to be 950 °C, in case of STEMET 1228 and 990 °C, in case of STEMET 1406. Both filler alloys had the same optimum brazing time which was 1800 s.

The fracture surfaces after the shear test were examined by X-ray diffraction. Figs. 9 and 10 display the XRD patterns for STEMET 1228 and STEMET 1406 samples, respectively. The XRD patterns demonstrated intense presence of Ti and Zr. Meanwhile, several intermetallic compounds were detected depending on the employed brazing parameters. At the brazing duration of 600 s (Figs. 9a and 10a), the dominating intermetallic phases were Ti_2Cu and Ti_2Ni for STEMET 1228, and Zr_2Cu for STEMET 1406. It could be concluded from the Ti–Zr–Cu ternary alloy phase diagram [30] that the Ti_2Cu or Ti_2Ni phases have some solubility of Zr. Therefore, the brazed joint consists of $(Ti,Zr)_2Cu$, $(Ti,Zr)_2Ni$ and β-Ti. Additionally, these phases were detected by SEM-EDS (Figs. 3 and 4, Tables 4 and 5). The Zr_2Ni intermetallic phase was clearly detected from fracture surfaces but with lower intensity, which might be due to their low volume fraction. When the brazing time was prolonged to

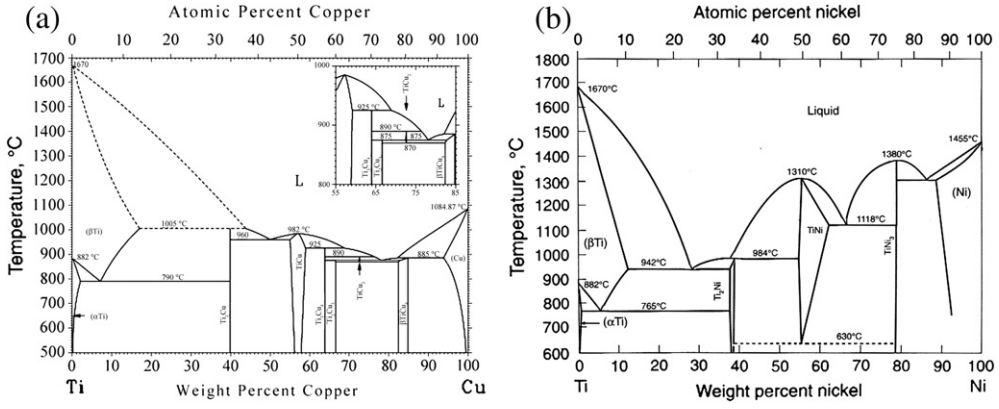

Fig. 5 – Binary alloy phase diagrams; (a) Ti–Cu and (b) Ti–Ni [26].

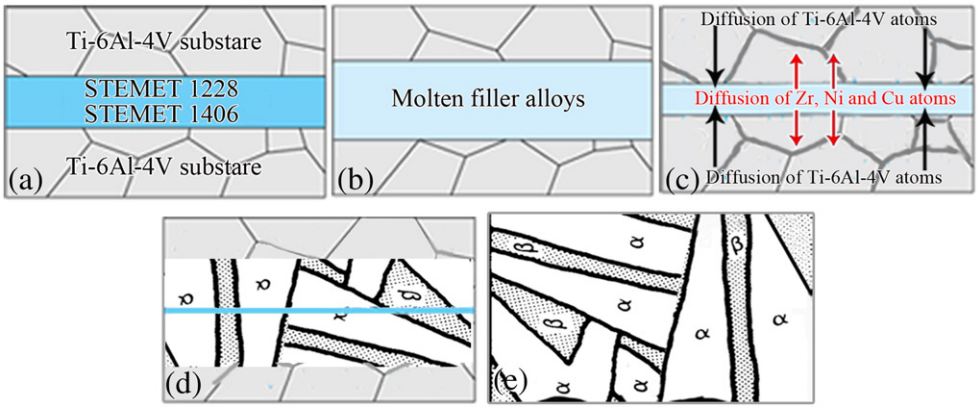

Fig. 6 – The model for describing the brazing process, (a) initial condition, (b) dissolution of filler alloy, (c) isothermal solidification, (d) homogenization and (e) developing Widmanstätten structure [27].

1200 s (Figs. 9b and 10b), almost all the intermetallic phases disappeared in the brazed joints, indicating almost complete solid solubility. These results clearly point to the crucial role of the interfacial layers in the bonding strength of the joints. The existence of Ti_2Cu, Ti_2Ni and Zr_2Cu phases strongly deteriorated the bonding strength of the furnace brazed joints [31].

Fig. 11 shows the SEM secondary electron image (SEI) fractographs of fractured surface of specimens furnace brazed at 950 °C in case of STEMET 1228 and 990 °C in case of STEMET 1406 by 1200 s duration time brazing. The hard and brittle intermetallic compounds (Ti_2Cu, Ti_2Ni and/or Zr_2Cu) at titanium interface were the main reasons for the crack initiation. During stress application in shear test, cracks prefer to propagate at the brittle intermetallic compounds and spread easily through them. An easy propagation of the crack leads to a decrease in the strength of the joints and the fracture behavior is likely to show cleavage morphology with facet characteristic. The shear strength measurements and the fracture behaviors recommended that the presences of Cu–Ni and Cu–Ni–Zr rich Ti phases in the brazed joint are detrimental and they should be avoided for obtaining sound joint.

Microhardness indentation measurements were also performed to evaluate the joints for both filler alloys as shown in Fig. 12. At the center regions for the 600 s samples (Fig. 12a

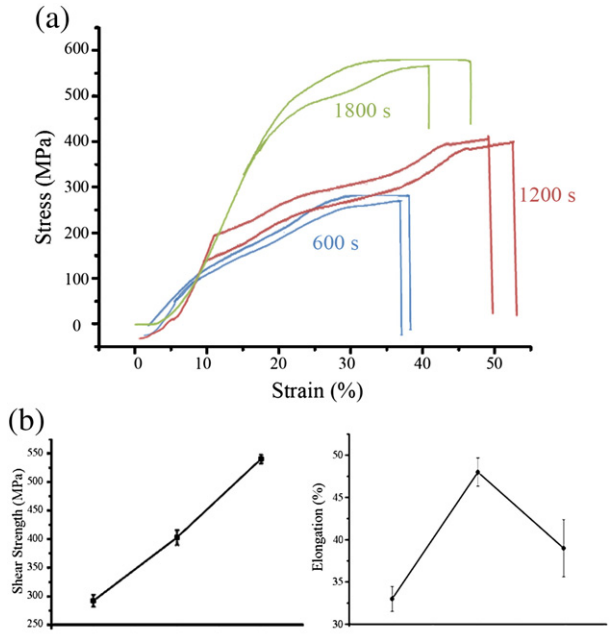

	Shear Strength (MPa)	Elongation (%)
950 °C - 600 s	292 ± 10	33 ± 2
950 °C - 1200 s	403 ± 13	48 ± 2
950 °C - 1800 s	540 ± 8	39 ± 3

Fig. 7 – (a) Shear stress–strain curves for the samples brazed with STEMET 1228 at temperature of 950 °C for 600, 1200 and 1800 s, (b) extrapolated mechanical properties from shear stress–strain curves (mean ± S.D.).

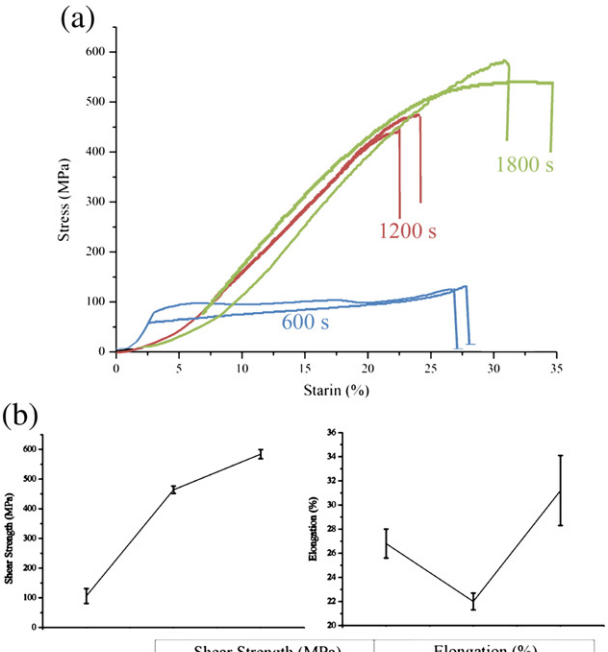

	Shear Strength (MPa)	Elongation (%)
950 °C - 600 s	106 ± 25	26.8 ± 1
950 °C - 1200 s	464 ± 12	22 ± 1
950 °C - 1800 s	584 ± 15	31.2 ± 2

Fig. 8 – (a) Shear stress–strain curves for the samples brazed with STEMET 1406 at temperature of 990 °C for 600, 1200 and 1800 s, (b) extrapolated mechanical properties from shear stress–strain curves (mean ± S.D.).

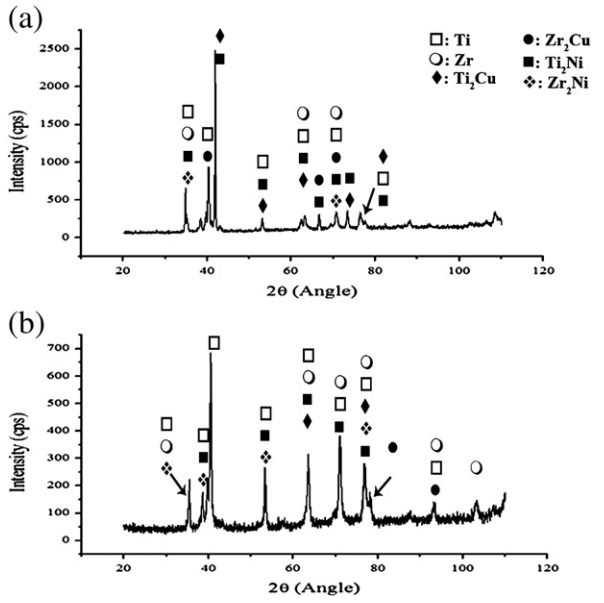

Fig. 9 – XRD patterns from fractured surfaces which brazed with STEMET 1228 at brazing temperatures of 950 °C for (a) 600 and (b) 1200 s.

and c), respective hardness values of around 1010 and 720 HV indicated the same as those of the original filler alloys, i.e., very hard and brittle phases. Intermetallic compounds established at interface regions showed the highest hardness values. The high hardness of the intermetallic compounds at the center of brazed joints reduces the ductility and hence the allowable plastic deformations, which contributed to decreasing the shear strength of the joints [32]. These zones were demonstrated sensitive to initiation of cracks during loading in the shear test as discussed earlier. Between the center regions and the base material, the respective hardness values were lower (840 and 625 HV) and they almost linearly decreased until the base material. On the other hand, both samples which brazed for 1800 s (Fig. 12b and d), showed much less variation in their microhardness profiles across the entire joint areas. It is also important to note that the acicular $\alpha+\beta$ phases at the vicinity of the interfaces had higher hardness values (~570 HV) than the equiaxed $\alpha+\beta$ Ti–6Al–4V base material (~491 HV). Acicular phases are harder than the equiaxed phases [2]. Therefore, developing an acicular Widmanstätten microstructure is much more useful for improving the mechanical properties. This is another reason for the increase in joint strength equal (or even superior) to the strength of the base material.

These results demonstrate that applying STEMET 1228 and STEMET 1406 amorphous filler alloys for brazing Ti-based materials generates superior mechanical properties at the brazed joints. Both brazing filler alloys have lower brazing temperature and higher shear strength than Cu-based filler alloy like Cu–12Mn–2Ni (wt.%) [33]. Therefore, this brazing process has a great potential to replace the welding techniques currently in practice for Ti-based materials.

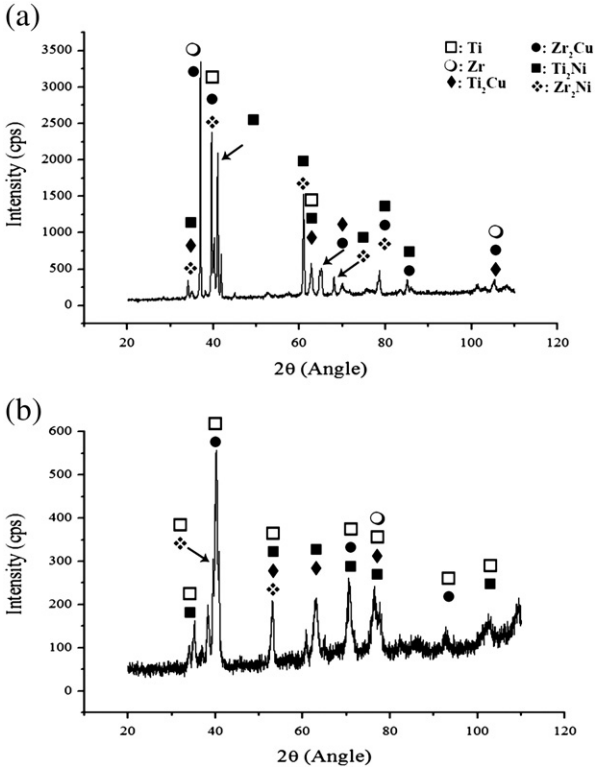

Fig. 10 – XRD patterns from fractured surfaces which brazed with STEMET 1406 at brazing temperatures of 990 °C for (a) 600 and (b) 1200 s.

4. Conclusions

The brazing of Ti–6Al–4V alloy using STEMET 1228 and STEMET 1406 filler foils was investigated for microstructural and mechanical properties and some drawn conclusions are summarized as following:

1- Brazed joints achieved at lower brazing time (600 s) contained three regions (or layers). One was an untransformed β layer in which some α phase nucleates from the base material. The second layer was Ti-rich phase with V, Ni, Cu and Al (transformed β) and the third is a segregated layer containing Zr–Cu–Ni-rich phase having the same chemical composition as the original filler alloy. Increasing the brazing time resulted in a decrease in the segregated region and finally it disappeared and substituted with a Widmanstätten structure by completing the eutectoid reaction.
2- The average shear strength of brazed joints increased with increasing the brazing time. Brazing with STEMET 1228 and STEMET 1406 at 950 °C and 990 °C, respectively for 1800 s demonstrated shear strengths as high as the strength of the base material. Developing the Widmanstätten structure at the entire joint area was the main cause for the increasing of the braze/joint strengths.
3- Based on the XRD results from fracture surfaces, and microhardness tests from cross sections of the brazed joints, the existence of hard intermetallic compounds such as Ti_2Cu, Ti_2Ni and Zr_2Cu were confirmed and they were the main reason for the deterioration of the shear strengths.

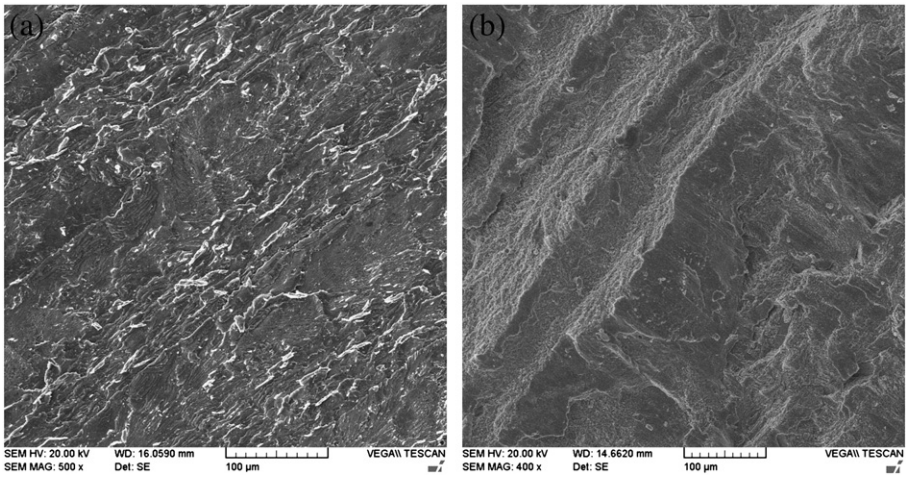

Fig. 11 – Fracture morphology of Ti–6Al–4V brazed joints at 950 °C–1200 s (STEMET 1228) and 990 °C–1200 s (STEMET 1409).

4- The brazed joints with low shear strength were fractured in the central brazed layer because of the brittleness of the intermetallic compounds existed in the central brazed layer with reciprocal brittle and quasi-cleavage morphology.
5- The joints brazed at 1800 s have normal microhardness distribution across the whole joint area. Therefore, developing an acicular Widmanstätten structure throughout the brazed joint is very suitable for the improvement of mechanical strength even equal to the strength of the base material.

Acknowledgment

The authors would like to thank the faculty of aerospace engineering for designing and manufacturing of brazing fixtures

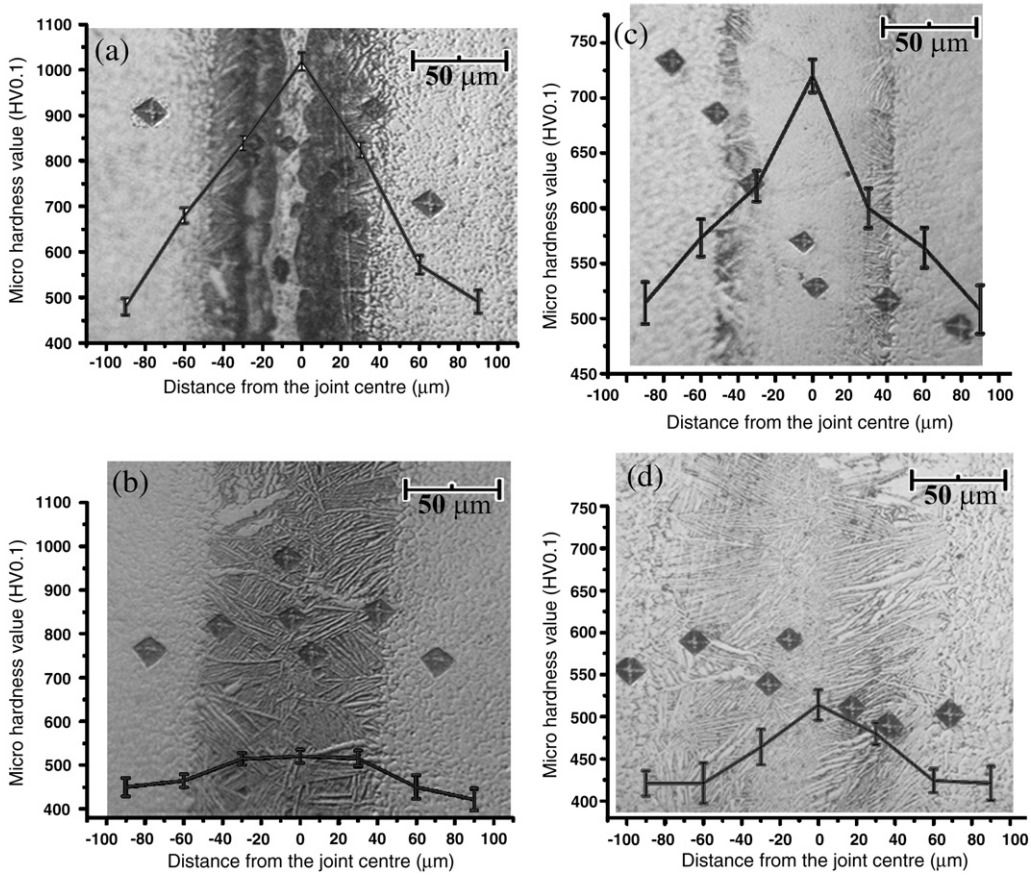

Fig. 12 – Microhardness test of different zones of Ti–6Al–4V/STEMET 1228 at temperature of 950 °C for (a) 600 and (b) 1800 s and Ti–6Al–4V/STEMET 1406 at temperature of 990 °C for (c) 600 and (d) 1800 s (mean ± S.D.).

and the air line of Islamic republic of Iran (Iran Air) for cooperation and providing the experimental facilities. Also, we are grateful of the physical and mechanical properties laboratory in the faculty of biomedical engineering at AUT. The authors would like to thank Dr. M. H. Siadati and Dr. A. Zolriasatein for their kind scientific editions on the preparation of this manuscript.

REFERENCES

[1] Liaw DW, Wu ZY, Shiue RK, Chang CS. Infrared vacuum brazing of Ti–6Al–4V and Nb using the Ti–15Cu–15Ni foil. Mater Sci Eng A 2007;454–455:104–13.
[2] Mj Donachie. Titanium: a technical guide. 2 ed. USA: ASM; 2000.
[3] Leyens C, Peters M. Titanium and titanium alloys fundamentals and applications. WILEY-VCH Verlag GmbH; 2003.
[4] Lutjering G, Williams JC. Titanium. 2 ed. Berlin: Springer; 2007.
[5] Yue X, He P, Feng JC, Zhang JH, Zhu FQ. Microstructure and interfacial reactions of vacuum brazing titanium alloy to stainless steel using an AgCuTi filler metal. Mater Charact 2008;59:1721–7.
[6] Elrefaey A, Tillmann W. Effect of brazing parameters on microstructure and mechanical properties of titanium joints. J Mater Process Technol 2009;209:4842–9.
[7] Huang X, Richards NL. Activated diffusion brazing technology for manufacture of titanium honeycomb structures — a statistical study. Suppl Weld J 2004:73–81.
[8] Shapiro AE, Flom YA. Brazing of titanium at temperatures below 800 °C: review and prospective applications. In: Proceedings of 8th International Conference in Brazing, High Temperature Brazing and Diffusion Welding; 2007. p. 254–67. Aachen, Germany.
[9] Shapiro A, Rabinkin A. State of the art of titanium-based brazing filler metals. Weld J October 2003:36–43.
[10] Tillmann W, Lugscheider E, Xu R, Indacochea JE. Kinetic and microstructural aspects of the reaction layer at ceramic/metal braze joints. J Mater Sci 1996;31:445–52.
[11] Chang CT, Shiue RK. Infrared brazing Ti–6Al–4V and Mo using the Ti–15Cu–15Ni braze alloy. Int J Refract Met Hard Mater 2005;23:161–70.
[12] Chang CT, Wu ZY, Shiue RK, Chang CS. Infrared brazing Ti–6Al–4V and SP-700 alloys using the Ti–20Zr–20Cu–20Ni braze alloy. Mater Lett 2007;61:842–5.
[13] Du YC, Shiue RK. Infrared brazing of Ti–6Al–4V using two silver-based braze alloys. J Mater Process Technol 2009;209: 5161–6.
[14] Shiue RK, Wu SK, Chen YT, Shiue CY. Infrared brazing of Ti50Al50 and Ti–6Al–4V using two Ti-based filler metals. Intermetallics 2008;16:1083–9.
[15] Chang CT, Du YC, Shiue RK, Chang CS. Infrared brazing of high-strength titanium alloys by Ti–15Cu–15Ni and Ti–15Cu–25Ni filler foils. Mater Sci Eng A 2006;420:155–64.
[16] Hong IT, Koo CH. Microstructural evolution and shear strength of brazing C103 and Ti–6Al–4V using Ti–20Cu–20Ni–20Zr (wt.%) filler metal. Int J Refract Met Hard Mater 2006;24:247–52.
[17] JIS Z 3192. Methods for tension and shear tests for brazed joint; 1988.
[18] Elrefaey A, Tillmann W. Interface characteristics and mechanical properties of the vacuum-brazed joint of titanium-steel having a silver-based brazing alloy. Metall Mater Trans A 2007;38:2956–62.
[19] Ganjeh E, Sarkhosh H, Khorsand H, Sabet H, Dehkordi EH, Ghaffari M. Evaluate of braze joint strength and microstructure characterize of titanium-CP with Ag-based filler alloy. Mater Des 2012;39:33–41.
[20] AWS C3.8. Recommended practice for ultrasonic inspection of brazed joints; 1997.
[21] Metals hand book, vol 9: metallography and microstructures. USA: ASM; 1998.
[22] Bakhtiari R, Ekrami A. Transient liquid phase bonding of FSX-414 superalloy at the standard heat treatment condition. Mater Charact 2012;66:38–45.
[23] ASTM, E384. Standard test method for microindentation hardness of materials; 2002.
[24] Chang E, Chen CH. Low-melting-point titanium-base brazing alloys—part 2: characteristics of brazing Ti.21Ni–14Cu on Ti–6Al–4V substrate. JMEPEG 1997;6:797–803.
[25] Doherty KJ, Tice JR, Szewczyk ST, Gilde GA. Titanium brazing for structures and survivability. Proceedings of the 3rd International Brazing and Soldering Conference; 2006. p. 268–73. San Antonio, Texas, USA.
[26] Metals hand book, vol 3: alloy phase diagrams. ASM; 1992.
[27] Schwartz MM. Brazing. 2 ed. USA: ASM; 2003.
[28] Lee JG, Choi YH, Lee JK, Lee GJ, Lee MK, Rhee CK. Low-temperature brazing of titanium by the application of a Zr–Ti–Ni–Cu–Be Bulk Metallic Glass (BMG) alloy as a filler. Intermetallics 2010;18:70–3.
[29] Dieter GE. Mechanical metallurgy. 3 ed. USA: McGraw Hill; 2001.
[30] Materials Science International Team M. Ternary alloy systems: phase diagrams, crystallographic and thermodynamic data, volume 11. Berlin, Germany: Springer; 2007.
[31] Shiue RK, Wu SK, Chan CH. The interfacial reactions of infrared brazing Cu and Ti with two silver-based braze alloys. J Alloys Compd 2004;372:148–57.
[32] Elrefaey A, Tillmann W. Correlation between microstructure, mechanical properties, and brazing temperature of steel to titanium joint. J Alloys Compd 2009;487:639–45.
[33] Elrefaey A, Tillmann W. Brazing of titanium to steel with different filler metals: analysis and comparison. J Mater Sci 2010;45:4332–8.